RSC Advances

PAPER

View Article Online
View Journal | View Issue

Cite this: *RSC Adv.*, 2023, **13**, 18812

Received 11th May 2023
Accepted 14th June 2023

DOI: 10.1039/d3ra03136e

rsc.li/rsc-advances

Influence of the physical properties of the layered oxyselenides $Bi_2YO_4Cu_2Se_2$ through Ni doping

Lin Xu,[a] Jingyuan Wu,[b] Zhidong Liu,[c] Weiao Kong,[c] Chuanhe Wang,[c] Yani Zhang[c] and Shugang Tan *[c]

We have synthesized a series of Ni-doped layered oxyselenides $Bi_2YO_4Cu_{2-x}Ni_xSe_2$ ($0 \le x \le 0.4$). The crystal structure and physical properties were studied through X-ray diffraction, and electric and thermo transport measurements. We also performed DFT calculations to study the electric structure of the designed $Bi_2YO_4Ni_2Se_2$, which is similar to that of KNi_2Se_2.

Introduction

In recent decades, compounds with layered crystal structures have attracted people's increasing attention due to their interesting physical properties, such as superconductivity,[1–3] charge density wave,[4–9] topological insulation[10] *etc.* In particular, the discovery of iron-based superconductors in 2008 aroused wide concern all over the world.[2] Up to now, the mechanism of high-temperature superconductivity remains a mystery, which requires the joint efforts of theoretical and experimental researchers. According to previous research experience, high-temperature superconductors tend to adopt layered crystal structures. And it has been an important way to search for new superconductors through exploring new layered compounds.

Among the known iron-based superconductors, they all have the Fe_2Pn_2/Fe_2Ch_2 (Pn = P, As; Ch = S, Se, Te) conducting layer, which is believed playing an important role in the superconductivity. In fact, all the iron-based superconductors have analogues in CuCh based compounds. For example, the 1111-type LaOFeP/As and LaOCuS/Se adopt the same crystal structure.[11,12] The 122-type KFe_2Se_2 and KCu_2Se_2, the 32 522-type $Sr_3Sc_2O_5Fe_2As_2$ and $Sr_3Sc_2O_5Cu_2S_2$ *etc.* All have the same situations.[13–15] Many iron-based superconductors were discovered by substituting Fe_2Pn_2 layers for Cu_2Ch_2 layers in the known CuCh-based compounds. In 2002, a new layered CuSe-based compound $Bi_2YO_4Cu_2Se_2$ was reported and we studied the physical and electric properties lately.[16–18] The Cu_2Se_2 layer is defined as the conducting layer and the Bi_2YO_4 layer is defined as the block layer. As every block layer provide one electron to conducting layer, which causes a mixed state of Cu^{2+}/Cu^{+}, it exhibits p-type metallic behaviour which is rare in CuCh-based compounds. Similarly, p-type metallic ground state is also found in KCu_2Se_2, in which the K layer also provides one electron to Cu_2Se_2 layer per unit cell. In 2012, the analogue KNi_2Se_2 was reported superconducting below 0.8 K, which has aroused people's extensive research interest.[19] If the Cu_2Se_2 layer in $Bi_2YO_4Cu_2Se_2$ was replaced by Fe_2Pn_2 or Ni_2Pn_2 layers, we think new superconductors may be achieved. We try our best to synthesize $Bi_2YO_4Ni_2Se_2$ through solid state reaction. Unfortunately, all the attempts ended in failure. On the other hand, it is also valuable to study the influence of the physical proper-ties of the layered oxyselenide $Bi_2YO_4Cu_2Se_2$ through Ni doping at Cu site. In this paper, we successfully doped 20% Ni at Cu site in $Bi_2YO_4Cu_2Se_2$. The temperature coefficient of resistivity can be effectively adjusted through Ni doping. Furthermore, we studied the thermoelectric properties of the Ni-doped samples. Finally, we study the electric structure of the designed $Bi_2YO_4Ni_2Se_2$ through the first principle calculation, which exhibit similar electronic structure with KNi_2Se_2. This will tempt people to explore the synthesis of $Bi_2YO_4Ni_2Se_2$ through other methods.

Results and discussion

The crystal structure of $Bi_2YO_4Cu_2Se_2$ is shown in Fig. 1(a), which is alternatively stacked by Bi_2YO_4 layer and Cu_2Se_2 layer. Fig. 1(b) shows the crystal structure of KNi_2Se_2, which has the $ThCr_2Si_2$-type structure.[20] Comparing these two structures, it is not difficult to find that their crystal structure is the same except the block layer. Fig. 2 shows the X-ray diffraction patterns of $Bi_2YO_4Cu_{2-x}Ni_xSe_2$. All the diffraction peaks of the doped samples match the Bragg peaks of $Bi_2YO_4Cu_2Se_2$, which indicates high quality samples. The fitting lattice parameters of $Bi_2YO_4Cu_{2-x}Ni_xSe_2$ are shown in Fig. 2(b). The lattice parameter *a* and *c* for $Bi_2YO_4Cu_2Se_2$ are 3.862 and 24.31 Å respectively, which is corresponding to previous results.[16,17] The lattice parameter a is decreased with increasing Ni content, while the lattice parameter *c* is the opposite. It indicates that the in-plane

[a]*Yantai Gold College, Yantai 265401, People's Republic of China*
[b]*Longkou No. 1 High School of Shandong Province, Yantai 265401, People's Republic of China*
[c]*School of Physics and Optoelectronic Engineering, Shandong University of Technology, Zibo 255000, People's Republic of China. E-mail: tanshugang@sdut.edu.cn*

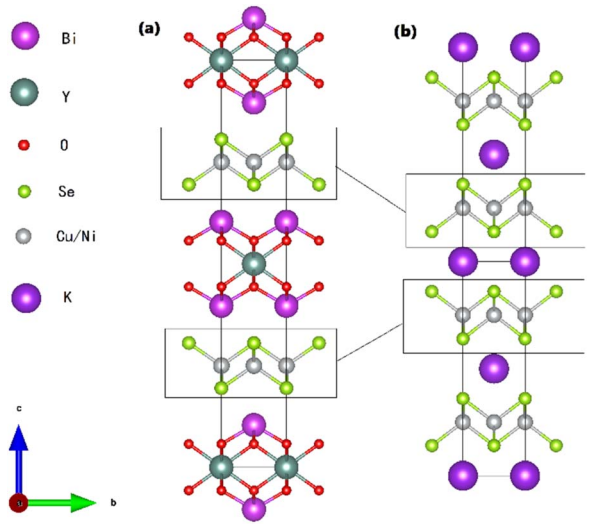

Fig. 1 The crystal structure of $Bi_2YO_4(Cu,Ni)_2Se_2$ (a) and KNi_2Se_2 (b).

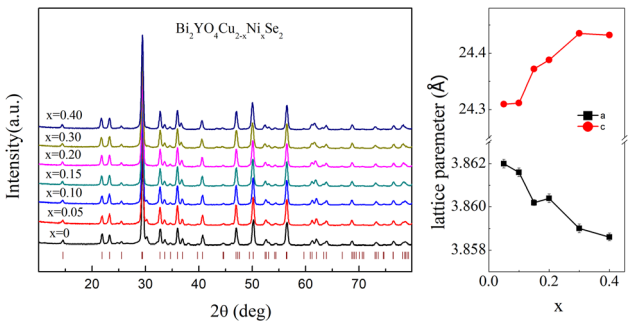

Fig. 2 The X-ray diffraction patterns and the fitted lattice parameters of $Bi_2YO_4Cu_{2-x}Ni_xSe_2$ measured at 300 K.

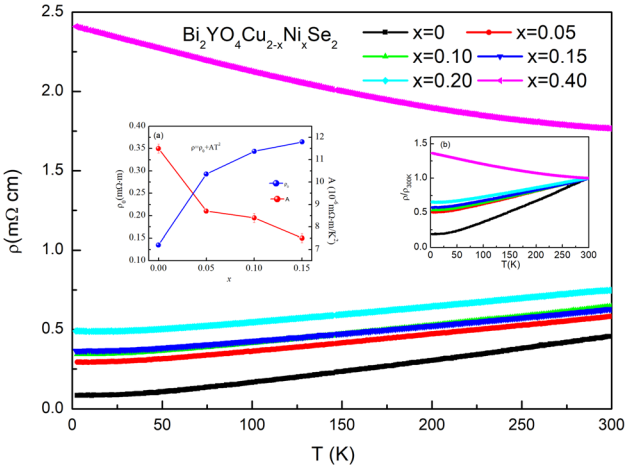

Fig. 3 The temperature dependence of the resistivity of $Bi_2YO_4Cu_{2-x}Ni_xSe_2$ from 2 to 300 K. Inset (a) is the parameter ρ_0 and A fitted through the Fermi liquid behavior equation with different Ni con-tent. Inset (b) is the reduced resistivity of $Bi_2YO_4Cu_{2-x}Ni_xSe_2$.

interaction is strengthened and the interlayer interactions are weakened. The reported lattice parameters a and c of KCu_2Se_2 are 4.008 and 13.643 Å respectively.[21] Compared with KCu_2Se_2, the thicker block layer in $Bi_2YO_4Cu_2Se_2$ makes the parameter a smaller. In other words, the in-plane interaction of $Bi_2YO_4Cu_2Se_2$ is stronger than that of KCu_2Se_2. For KNi_2Se_2, the fitted lattice parameter a and c according to experiment result are 3.89295 and 13.3158 Å respectively and the calculated lattice parameter a and c according to DFT calculation are 3.9680 and 13.0479 Å respectively.[19,20,22] The lattice parameter a of KNi_2Se_2 is larger than that of $Bi_2YO_4Cu_2Se_2$. According to the above results, the lattice parameter a of $Bi_2YO_4Ni_2Se_2$, if it exists, should be larger than that of KNi_2Se_2. This may be the reason we cannot doped much more Ni in $Bi_2YO_4Cu_2Se_2$.

Fig. 3 shows the temperature dependence of the electric resistivity of $Bi_2YO_4Cu_{2-x}Ni_xSe_2$. For $Bi_2YO_4Cu_2Se_2$, the resistivity increases with increasing temperature from 2 to 300 K, which indicates a metallic transport behaviour and is similar with previous results.[17] The value of resistivity is increased with increasing Ni content. Compared with KNi_2Se_2, the resistivity is relatively higher. Unfortunately, no superconducting behaviour was found until 2 K for all the Ni doped $Bi_2YO_4Cu_2Se_2$. According to previous study,[17] the metallic behaviour originates from the mixed valences of Cu ion in Cu_2Se_2 layer. Every Bi_2YO_4 unit provides one electron to Cu_2Se_2 unit, so every two Cu atoms only pro-vide 3 electrons to keep balance. While when Ni is doped at Cu site, every Ni atom can provide two electrons, namely electronic doping. For undoped $Bi_2YO_4Cu_2Se_2$, the carriers are mainly p-type. Regardless of other factors, Ni doping at Cu site decreases the carrier con-centration and the resistivity would increase with increasing Ni content. Our experimental results are consistent with the viewpoint. As shown in Fig. 3, the reduced resistivity increases with increasing Ni content. Furthermore, the $Bi_2YO_4Cu_{1.6}Ni_{0.4}Se_2$ exhibits semiconducting/insulating transport behaviour from 2 to 300 K. The resistivity ($x = 0$–0.2) obey the Fermi liquid behaviour from 2 K to 50 K. We fitted the resistivity curves through the Fermi liquid behaviour equation $\rho = \rho_0 + AT^2$. Where ρ_0 represents the residual resistivity. The results are shown in the inset (a) of Fig. 3. As can be seen, the residual resistivity in-creases with x. As known, the residual resistivity ρ_0 is in direct proportion to $m^*\hbar/n\tau_0$, where m^*, n and $\hbar/\tau_0$ represent the carrier effective mass, carrier concentration and the scattering rate related to the disordered potential. For $Bi_2YO_4Cu_{1.6}Ni_{0.4}Se_2$, it exhibits semiconducting transport behaviour that the resistivity decreases with arising temperature. Further study is needed to clarify the ground state of Ni doped $Bi_2YO_4Ni_2Se_2$. According to previous study, the ground state of KNi_2Se_2 is metallic.[20] Our following DFT calculation result also indicates the metallic ground state of $Bi_2YO_4Ni_2Se_2$. It should not turn it to semiconductor through Ni doping. The semiconducting-like phenomenon should not be intrinsic, which may be caused by defect or grain boundary introduced with Ni doping.

Fig. 4 shows the thermoelectric properties of $Bi_2YO_4Cu_{2-x}Ni_xSe_2$ ($x = 0$, 0.2, 0.3). Fig. 4(b) shows the Seebeck coefficient curves of $Bi_2YO_4Cu_{2-x}Ni_xSe_2$. The Seebeck coefficient also exhibits metallic behaviour from 100 to 300 K, increasing with temperature linearly according to the equation

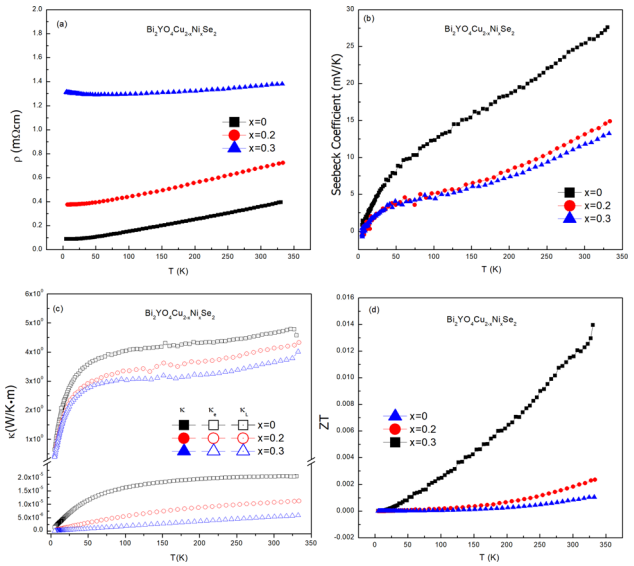

Fig. 4 The thermoelectric properties of $Bi_2YO_4Cu_{2-x}Ni_xSe_2$.

$$S = \frac{8\pi^2 k_B{}^2 Tm^*}{3eh^2}\left(\frac{\pi}{3n}\right)^{2/3}$$

where k_B is the Boltzmann constant, m^* is the effective mass of carrier, and n is the carrier concentration, which applies for metals or degenerate semiconductors under assumption of parabolic band and acoustic phonon scattering approximation. The Seebeck coefficients are positive for all the samples ranging from 5 to 330 K, indicating p-type carriers dominated in these materials, which is consistent with previous results. The Seebeck coefficient decreases with increasing Ni content. Fig. 3(c) shows the total thermal conductivity curves. The total thermal conductivity decreases with increasing Ni content. The total thermal conductivity can be divided into the electron component (κ_e) and the lattice component (κ_l): $\kappa = \kappa_e + \kappa_l$. The electron component is proportional to the electrical conductivity according to Wide–Franz law, $\kappa_e = L\sigma T = LT/\rho$. The decreasing resistivity indicates the electron component of the total thermal conductivity increase. Then the lattice thermal conductivity decreases with increasing Ni content, which originates from the increasing defect scattering induced by Ni. The dimensionless figure of merit is defined as $ZT = S^2/\rho\kappa T$, which is the measure of the efficiency of a thermoelectric material. We calculated the ZT of the synthesized samples, which is shown in Fig. 4(d). Although the induce of Ni de-crease the resistivity of the sample, the ZT decrease with increasing Ni content because of the great degree reduction of the Seebeck coefficient. The introduction of Ni is unfavourable to the improvement of thermoelectric properties in $Bi_2YO_4Cu_2Se_2$.

The plane-wave projector augmented method as implement in the Vienna *ab initio* simulation package (VASP) was used to calculate the density of states (DOS) and energy band. The Perdew–Bruke–Ernzerhof (PBE) form of generalized gradient approximation (GGA) was chosen as the exchange–correlation potential.[23] Due to the ex-change–correlation effects of the strongly localized Cu and Ni 3d electrons, we adopted the DFT + U method. We tested different values of the screened Coulomb parameter U. The added Coulomb interactions do not change the ground state. An energy cut-off of 520 eV was used in all cases. The convergence criterion for energy was set to be 10^{-6} eV per unit cell and the forces on all relaxed atoms were less than 0.01 eV A^{-1}. According to previous study, nonmagnetic states is adopted to calculate the electronic band structure. Fig. 5 shows the band structure of $Bi_2YO_4Cu_2Se_2$ and $Bi_2YO_4Ni_2Se_2$. The calculated band structure of $Bi_2YO_4Cu_2Se_2$ is consistent to previous result. The Fermi energy located at the valence band, indicating the p-type metallic ground state, which is consistent with the experiment results. Furthermore, as the replace of Cu by Ni, the Fermi energy move deeper in valence band, namely similar p type metallic ground state. The conduction band is attached to the valence band. The semiconducting behaviour in Ni-doped $Bi_2YO_4Cu_2Se_2$ observed in our experiment may be non-intrinsic. For $Bi_2YO_4Cu_2Se_2$, the bands exhibit complicated character near the Fermi surface. Along the Z–Γ line, the energy dispersion is very weak. The energy dispersion is strong in the layer-parallel directions, which originates from the strong hybridizations between Cu and Se. Similar quasi-two-dimensional properties are found in $Bi_2YO_4Ni_2Se_2$, which is consistent with KNi_2Se_2.[20] There are also two bands crossing the Fermi energy, indicting the multi-band character. Compared the band structure of $Bi_2YO_4Ni_2Se_2$ and KNi_2Se_2, the structure of the valence band is very similar. Moreover, the thick Bi_2YO_4 layer make the 2D property more obvious. The $ThCr_2Si_2$-type super-conductor KNi_2Se_2 was discovered with a super-conducting transition temperature of 0.8 K. We believe the $Bi_2YO_4Cu_2Se_2$ may be a superconducting material if it can be successful synthesized.

Experimental

$Bi_2YO_4Cu_{2-x}Ni_xSe_2$ sample was prepared by reacting a stoichiometric mixture of Bi_2O_3, Y_2O_3, Y, Cu, Ni and Se. The raw materials weighed by stoichiometric ratio were mixed. After thoroughly grounding in an agate pestle and mortar, the mixtures were pressed into pellets under 12 MPa. The pellets

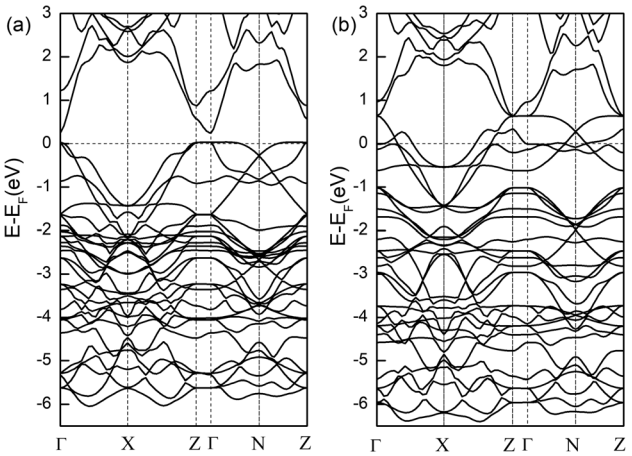

Fig. 5 The band structure of $Bi_2YO_4Cu_2Se_2$ and $Bi_2YO_4Ni_2Se_2$.

were then sealed under vacuum ($<10^{-4}$ Pa) in the silica tubes which had been baked in drybox for 1–2 h at 150 °C. The ampoules were heated to 830 °C and maintained at this temperature for 24 h. Finally, the furnace is shut down and cools to room temperature naturally. The obtained samples were reground, pelletized, and heated for another 24 hours at 830 °C followed by furnace cooling. The X-ray powder diffraction patterns were recorded at room temperature on a PANalytical diffractometer (X'Pert PRO MRD) with Cu Kα radiation (40 kV, 40 mA). Structural refinement of powder samples was carried out by using Rietica software. The electrical resistivity and thermoelectric properties were measured using a Quantum Design PPMS (Physical Properties Measurement System) from 300 to 2 K.

Conclusions

In summary, we have synthesized a series of layered oxyselenides $Bi_2YO_4Cu_{2-x}Ni_xSe_2$ through solid state reaction. There crystalline structures and physical properties were thoroughly studied. Along with the increase of Ni content, the resistivity increase. It exhibits semiconducting transport behaviour in $Bi_2YO_4Cu_{1.6}Ni_{0.4}Se_2$, which may be caused by the diffraction of impurity or defects. The crystal structure and band structure of $Bi_2YO_4Ni_2Se_2$ are like those of KNi_2Se_2. We suspect that $Bi_2YO_4Ni_2Se_2$ should also exhibit superconductivity if it can be successfully synthesized.

Author contributions

Conceptualization, L. X. and J. W.; methodology, L. X.; validation, Z. L., W. K. and C. W.; formal analysis, Y. Z.; investigation, S. T.; resources, S. T.; data curation, L. X.; writing—original draft preparation, S. T.; writing—review and editing, L. X.; all authors have read and agreed to the published version of the manuscript.

Conflicts of interest

There are no conflicts to declare.

Acknowledgements

This work was supported by the Research Start-up Funds of Shandong University of Science and Technology (No. 415058).

Notes and references

1 J. Chen, L. Hu, J. X. Deng and X. R. Xing, *Chem. Soc. Rev.*, 2015, **44**, 3522.
2 Y. Kamihara, T. Watanabe, M. Hirano and H. Hosono, *J. Am. Chem. Soc.*, 2008, **130**, 3296.
3 Y. Mizuguchi, S. Demura, K. Deguchi, Y. Takano, H. Fujihiss, Y. Gotoh, H. Izawa and O. Miura, *J. Phys. Soc. Jpn.*, 2012, **81**, 114725.
4 F. Weber, S. Rosenkranz, J. P. Castellan, R. Osborn, R. Hott, R. Heid, K. P. Bohnen, T. Egami, A. H. Said and D. Reznik, *Phys. Rev. Lett.*, 2011, **107**, 107403.
5 L. P. Gor'kov, *Phys. Rev. B: Condens. Matter Mater. Phys.*, 2012, **85**, 165142.
6 X. Xi, Z. Wang, W. Zhao, J. H. Park, K. T. Law, H. Berger, L. Forró, J. Shan and K. F. Mak, *Nat. Phys.*, 2016, **12**, 139.
7 Y. Yang, S. Fang, V. Fatemi, J. Ruhman, E. Navarro-Moratalla, K. Watanabe, T. Taniguchi, E. Kaxiras and P. Jarillo-Herrero, *Phys. Rev. B*, 2018, **98**, 035203.
8 E. Navarro-Moratalla, J. O. Island, S. Mañas-Valero, E. PinillaCienfuegos, A. Castellanos-Gomez, J. Quereda, G. RubioBollinger, L. Chirolli, J. A. Silva-Guillén, N. Agraït, G. A. Steele, F. Guinea, H. S. J. van der Zant and E. Coronado, *Nat. Commun.*, 2016, **7**, 11043.
9 S. C. de la Barrera, M. R. Sinko, D. P. Gopalan, N. Sivadas, K. L. Seyler, K. Watanabe, T. Taniguchi, A. W. Tsen, X. Xu, D. Xiao and B. M. Hunt, *Nat. Commun.*, 2018, **9**, 1427.
10 S. Murakami, N. Nagaosa and S.-C. Zhang, Spin-Hall insulator, *Phys. Rev. Lett.*, 2004, **93**, 156804.
11 Y. Kamihara, T. Watanabe, M. Hirano and H. Hosono, *J. Am. Chem. Soc.*, 2008, **130**, 3296.
12 Y. Kamihara, H. Hiramatsu, M. Hirano, R. Kawamura, H. Yanagi, T. Kamiya and H. Hosono, *J. Am. Chem. Soc.*, 2006, **128**, 10012.
13 M.-L. Liu, L.-B. Wu, F.-Q. Huang, L.-D. Chen and I.-W. Chen, *J. Appl. Phys.*, 2007, **102**, 116108.
14 D. O. Scanlon and G. W. Watson, *Chem. Mater.*, 2009, **21**, 5435.
15 O. Tiedje, E. E. Krasovskii, W. Schattke, P. Stoll, C. Nather and W. Bensch, *Phys. Rev. B: Condens. Matter Mater. Phys.*, 2003, **67**, 134105.
16 J. S. O. Evans, E. B. Brogden, A. L. Thompson and R. L. Cordiner, *Chem. Commun.*, 2002, 912.
17 S. G. Tan, D. F. Shao, W. J. Lu, B. Yuan, Y. Liu, J. Yang, W. H. Song, H. Lei and Y. P. Sun, *Phys. Rev. B: Condens. Matter Mater. Phys.*, 2014, **90**, 085144.
18 Y. Yang, J. Han, Z. Zhou, M. Zou, Y. Xu, Y. Zheng, C.-W. Nan and Y.-H. Lin, *Adv. Funct. Mater.*, 2022, **32**, 2113164.
19 R. N. James, L. Anna, V. S. Andreas, L. Wu, J. J. Wen, J. Tao, Y. M. Zhu, B. T. Zlatko, N. P. Armitage and M. M. Tyrel, *Phys. Rev. B: Condens. Matter Mater. Phys.*, 2012, **86**, 054512.
20 F. Lu, J. Z. Zhao and W.-H. Wang, *J. Phys.: Condens. Matter*, 2012, **24**, 495501.
21 O. Tiedje, E. E. Krasovskii, W. Schattke, P. Stoll, C. Näther and W. Bensch, *Phys. Rev. B: Condens. Matter Mater. Phys.*, 2003, **67**, 134105.
22 R. N. James and M. M. Tyrel, *J. Am. Chem. Soc.*, 2012, **134**, 7750.
23 F. Ahmed, N. Tsujii and T. Mori, *J. Mater. Chem. A*, 2017, **5**, 7545.